

Inference of Hierarchical Core–Periphery Structure in Temporal Networks

Theodore Y. Faust*

Department of Mathematics, University of California, Los Angeles, Los Angeles, CA, USA

Mason A. Porter

Department of Mathematics, University of California, Los Angeles, Los Angeles, CA, USA

Department of Sociology, University of California, Los Angeles, Los Angeles, CA, USA and

Santa Fe Institute, Santa Fe, NM, USA

(Dated: June 17, 2025)

Networks can have various types of mesoscale structures. One type of mesoscale structure in networks is core–periphery structure, which consists of densely-connected core nodes and sparsely-connected peripheral nodes. The core nodes are connected densely to each other and can be connected to the peripheral nodes, which are connected sparsely to other nodes. There has been much research on core–periphery structure in time-independent networks, but few core–periphery detection methods have been developed for time-dependent (i.e., “temporal”) networks. Using a multilayer-network representation of temporal networks and an inference approach that employs stochastic block models, we generalize a recent method for detecting hierarchical core–periphery structure [1] from time-independent networks to temporal networks. In contrast to “onion-like” nested core–periphery structures (where each node is assigned to a group according to how deeply it is nested in a network’s core), hierarchical core–periphery structures encompass networks with nested structures, tree-like structures (where any two groups must either be disjoint or have one as a strict subset of the other), and general non-nested mesoscale structures (where the group assignments of nodes do not have to be nested in any way). To perform statistical inference and thereby identify core–periphery structure, we use a Markov-chain Monte Carlo (MCMC) approach. We illustrate our method for detecting hierarchical core–periphery structure in two real-world temporal networks, and we briefly discuss the structures that we identify in these networks.

I. INTRODUCTION

In network analysis, it is common to study various types of mesoscale structures [2]. The best-known type of mesoscale structure is community structure, in which densely-connected sets of nodes are connected sparsely to other sets of densely-connected nodes [3]. Another well-known type of mesoscale structure is role structure, in which one seeks to assign nodes to roles based on similarities between the local network structures in their neighborhoods [4]. A third prominent type of mesoscale structure is core–periphery structure in which well-connected nodes (so-called “core” nodes) are connected densely to each other and potentially densely connected to other nodes (so-called “peripheral” nodes), which are connected sparsely to other nodes [5–7]. In the present paper, we examine core–periphery structure, in which well-connected nodes (so-called “core” nodes) are connected densely to each other and potentially densely connected to other nodes (so-called “peripheral” nodes), which are connected sparsely to other nodes [5–7]. Core–periphery structure has been studied in many time-independent networks in the past few decades, leading to insights into topics such as social networks [8, 9], academic networks [10, 11], economic networks [12, 13], transportation networks [14], and many other areas. In many situations — including in the analysis of the spread of diseases through

face-to-face contacts [15], transportation systems [16], and legislation cosponsorships [17, 18] — it is important to consider relationships and/or interactions that change with time. In such situations, one can study a time-dependent network (i.e., a “temporal network”) [19–21]. In a temporal network, the entities (i.e., the nodes) in a network and/or the ties (i.e., the edges) can change with time. One way to examine a temporal network is as a sequence of ordinary time-independent networks (i.e., monolayer networks) in which each network in the sequence encodes the relationships between entities during one time point or time period. One can study such a temporal network using a multilayer-network representation [22]. Many approaches have been developed to study community structure in time-dependent networks [1, 6, 23, 24], but there are only a few studies of core–periphery structure in multilayer networks. For example, Bergemann et al. used spectral methods to identify core–periphery structure in multilayer networks [25, 26], Nie et al. used a rich-club approach to identify core–periphery structure in multiplex networks [27], and Hashemi and Behrouz generalized the concept of k -cores to multiplex networks [28].

In the present paper, we study a hierarchical notion of core–periphery structure in temporal networks (which we represent as multilayer networks). We generalize the hierarchical core–periphery structure of Polanco and Newman [1] from ordinary networks (i.e., graphs) to temporal networks. This notion of hierarchical core–periphery structure encompasses a rich variety of possible mesoscale structures, including ones that are not nested. In a

* Contact author: tfaust@math.ucla.edu

nested (i.e., onion-like) core–periphery structure [24], each node of a network is part of exactly one group, with higher-numbered groups signifying nodes that are deeper into a core. In such a setting, the probability that there is an edge between two nodes depends on the lower of the two group assignments of those nodes. By contrast, in the hierarchical core–periphery structure in [1], each node of a network can be in several groups simultaneously. One determines the edge probability between two nodes using the highest-numbered group that includes both nodes. This hierarchical formulation allows the generation of networks with nested structure, tree-like structure (where any two groups must either be disjoint or have one be a strict subset of the other), and general non-nested mesoscale structures (where the group assignments of nodes do not have to be nested in any way).[29]

To identify hierarchical core–periphery structure in temporal networks, we use statistical inference. This makes our approach more computationally costly than spectral methods to detect core–periphery structure, but it also yields several important benefits [30]. For example, the use of statistical inference guarantees that posterior-sampling methods yield samples precisely from the specified posterior distribution in the limit as the number of nodes of a network goes to infinity. Indeed, we prove in this limit that the stable distribution of a slightly-modified version of the Markov-chain Monte Carlo (MCMC) approach that we use for statistical inference is the same as the desired posterior distribution. Additionally, in contrast to many other approaches, such as non-inferential optimization approaches, statistical-inference methods avoid identifying mesoscale structures in completely random networks, which (by construction) arise from models without any mesoscale structure [30].

After we discuss our approach and give reasons for various choices that we make, we use it to study two real-world temporal networks. These two example networks are a network of ties between terrorist organizations in the Indian states of Jammu and Kashmir [31] and a network of co-appearances in the *Luke Gospel* [32]. For each example, we show that the identified core–periphery structure is plausible.

Our paper proceeds as follows. In Section II, we introduce our main notation. In Section III, we present the details of the generative model that we use for statistical inference of hierarchical core–periphery structure. In Section IV, we present the MCMC approach that we use to identify such structure. In Section V, we discuss the consequences of the choice of generative model on the performance of our MCMC approach. In Section VI, we use our statistical-inference approach to identify hierarchical core–periphery structure in two real-world temporal networks. In Section VII, we conclude and discuss several future directions.

II. NOTATION

In this section, we introduce notation for both monolayer networks (i.e., ordinary graphs) and temporal networks, which we represent as multilayer networks in which each layer corresponds to one time step (which can represent a time point or time period) [22].

We first discuss our notation for monolayer networks. For simplicity, we consider unweighted and undirected networks without self-edges or multi-edges. A monolayer network is a graph $G = (V, E)$, which consists of a set $V = \{1, \dots, N\}$ of nodes (i.e., vertices) and a set $E \subseteq V \times V$ of edges. We denote an undirected edge by (i, j) . We represent a monolayer network G using an adjacency matrix $A \in \{0, 1\}^{n \times n}$, where $A_{ij} = 1$ if nodes i and j are connected directly by an edge (i.e., they are adjacent) and $A_{ij} = 0$ otherwise.

To represent a temporal network, we examine a multilayer network in which each layer encodes the adjacencies between the nodes at its associated time step. We model a temporal network as a sequence of network layers (i.e., times) $\ell \in \{1, \dots, L\}$. At each time $\ell \in \{1, \dots, L\}$, we consider all nodes $i \in \{1, \dots, n\}$. We refer to an instantiation of a node in a given layer as a node-layer $(i, \ell) \in \{1, \dots, n\} \times \{1, \dots, L\}$. We again use an adjacency representation, so we have a sequence $(A^{(1)}, \dots, A^{(L)})$, with $A^{(\ell)} \in \{0, 1\}^{n \times n}$ for each layer ℓ . We assume that the networks are unweighted and undirected, so $A_{ij}^{(\ell)} = 1$ if node-layers (i, ℓ) and (j, ℓ) are adjacent and $A_{ij}^{(\ell)} = 0$ if they are not adjacent. For notational convenience, we let A denote the sequence $(A^{(1)}, \dots, A^{(L)})$. Technically, this is an abuse of notation, because we already used A to refer to a single adjacency matrix for a monolayer network, but we always clearly state whether we are considering a monolayer network or a temporal network. As general terminology, we refer to A as an *adjacency structure*. For convenience (and despite the additional associated abuse of notation), we also sometimes refer to A as a “network”.

III. A HIERARCHICAL GENERATIVE MODEL FOR CORE–PERIPHERY STRUCTURE IN TEMPORAL NETWORKS

As in [1], we think of core–periphery structure as a hierarchy with groups of nodes that do not need to be nested. We allow each node-layer to be a member of each of k groups, which we label with the indices $0, 1, \dots, k - 1$. In our hierarchical core–periphery setting, the probability of an edge between two nodes is determined by the highest-numbered group that includes both nodes [1]. By contrast, in a nested core–periphery setting [24], researchers typically require each node of a network to be a member of exactly one group with indices in $0, 1, \dots, k - 1$. In the nested core–periphery setting, the probability that there is an edge between two nodes

depends on the lower of the two group assignments of the nodes.

To ensure that the hierarchical structure has a “base level”, we assume (as in [1]) that every node is in group 0. We define a set of indicator variables $g_{(i,\ell)}^r$, where $g_{(i,\ell)}^r = 1$ if node-layer (i,ℓ) is in group r and $g_{(i,\ell)}^r = 0$ otherwise.

To generate a temporal network A given group assignments g , we use the model in [1] independently for each layer. For each pair of node-layers $(i,\ell), (j,\ell)$ in the same layer, we place an edge between them independently with probability $\omega_{h((i,\ell),(j,\ell))}^{(\ell)} \in [0, 1]$, where $h((i,\ell), (j,\ell))$ is the highest common group that includes both nodes (i.e., the largest r such that $g_{(i,\ell)}^r = g_{(j,\ell)}^r = 1$). Applying the argument in equations (1)–(3) from Section II of [1], we then have

$$P(A|\omega, k, g) = \prod_{\ell=1}^L \prod_{r=0}^{k-1} \left[(\omega_r^{(\ell)})^{m_r^{(\ell)}} (1 - \omega_r^{(\ell)})^{t_r^{(\ell)} - m_r^{(\ell)}} \right],$$

where

$$t_r^{(\ell)} = \sum_{\substack{1 \leq i < j \leq n}} \delta_{r, h((i,\ell), (j,\ell))}$$

is the number of node-layer pairs $(i,\ell), (j,\ell)$ in layer ℓ that have highest common group r and

$$m_r^{(\ell)} = \sum_{\substack{1 \leq i < j \leq n}} A_{ij}^{(\ell)} \delta_{r, h((i,\ell), (j,\ell))}$$

is the number of such pairs that are adjacent to each other.

To avoid a dependence on the parameters $\omega_r^{(\ell)}$, we follow the approach in [1]. For all r and ℓ , we assume that there is a uniform prior $\mathbb{P}(\omega_r^{(\ell)}) = 1$. The computations in equation (4) of [1] show that marginalizing according to these choices of prior distributions yields

$$\mathbb{P}(A|k, g) = \prod_{\ell=1}^L \prod_{r=0}^{k-1} \frac{m_r^{(\ell)}! (t_r^{(\ell)} - m_r^{(\ell)})!}{(t_r^{(\ell)} + 1)!}. \quad (1)$$

We break the discussion of our model into two parts. In Section III A, we consider a variant of our model in which we fix the number k of groups. In Section III B, we remove this assumption and introduce our main model, in which the number k of groups is unspecified.

A. Fixed Number of Groups

Suppose that we fix the number k of groups. To perform Bayesian inference on a temporal network A to yield a posterior distribution $\mathbb{P}(g|A)$, we need a prior distribution $\mathbb{P}(g|k)$ for the group assignments of nodes. There are many possible choices, such as a uniform distribution over group assignments (i.e., $\mathbb{P}(g|k) \propto 1$) for such a prior distribution. However, Faust showed in [33] in the context of community structure that many common choices for this prior distribution, such as a uniform distribution and generating g via a discrete-time Markov process, make it prohibitively unlikely to obtain large or small groups, which typically is an undesirable situation. This, in turn, impacts the accuracy of statistical inference of small and large groups.

To mitigate the group-size bias, we determine group assignments using an approach that was developed in [33]. We start by selecting the group sizes for the first layer uniformly at random. Given these group sizes, we choose the group assignments of nodes uniformly at random from all group assignments with the chosen group sizes. In other words, we choose the group assignments $g_{(1)}$ of the nodes in the first layer according to the probability distribution

$$P(g_{(1)}|k) = \prod_{r=1}^{k-1} \frac{(n_1(g_{(1)}^r))! \times (n - n_1(g_{(1)}^r))!}{(n+1)!}, \quad (2)$$

where $n_1(g_{(1)}^r)$ is the number of nodes in layer 1 that have group- r indicator variables of 1.

To generate each layer beyond the first one, we use the group assignments from the previous layer to generate those in the next layer via the probability distribution

$$\mathbb{P}(g_{(\ell)}^r | g_{(\ell-1)}^r) = \prod_{s=0}^1 \left[\frac{1}{\binom{n_s(g_{(\ell-1)}^r)}{c_{r;ss}^{(\ell)}}} \times \int_0^1 p_{r;s,\ell}^{n_s(g_{(\ell-1)}^r) - c_{r;ss}^{(\ell)}} \frac{p_{r;s,\ell} - 1}{p_{r;s,\ell}^{n_s(g_{(\ell-1)}^r) + 1} - 1} dp_{r;s,\ell} \right], \quad (3)$$

where $g_{(\ell)}^r$ is the set of indicator variables of group r for all nodes in layer ℓ , the quantity $n_s(g_{(\ell-1)}^r)$ is the number of nodes in layer $\ell-1$ that have group- r indicator variables of s , the quantity $c_{r;ss}^{(\ell)}$ is the number of nodes i such

that $g_{(i,\ell-1)}^r = s$ and $g_{(i,\ell)}^r = s$, and each $p_{r;s,\ell}$ is the parameter of an independent geometric distribution [34].

For notational convenience, we define

$$J(k_1, k_2) = \int_0^1 x^{k_1} \frac{x-1}{x^{k_2+1} - 1} dx.$$

Using this notation, we can write (3) as

$$\mathbb{P}(g_{(\ell)}^r | g_{(\ell-1)}^r) = \prod_{s=0}^1 \left[\frac{1}{\binom{n_s(g_{(\ell-1)}^r)}{c_{r;ss}^{(\ell)}}} \times J(n_s(g_{(\ell-1)}^r) - c_{r;ss}^{(\ell)}, n_s(g_{(\ell-1)}^r)) \right]. \quad (4)$$

Finally, we set

$$\mathbb{P}(g|k) = \mathbb{P}(g_{(1)}) \prod_{\ell=2}^L \prod_{r=1}^{k-1} \mathbb{P}(g_{(\ell)}^r | g_{(\ell-1)}^r), \quad (5)$$

and we thereby obtain the prior distribution $\mathbb{P}(g|k)$. Using the notation

$$F(g|k) = \prod_{\ell=2}^L \prod_{r=1}^{k-1} \mathbb{P}(g_{(\ell)}^r | g_{(\ell-1)}^r), \quad (6)$$

we write (5) as

$$\mathbb{P}(g|k) = \mathbb{P}(g_{(1)}|k) F(g|k). \quad (7)$$

By Bayes' rule,

$$\mathbb{P}(g|A, k) = \frac{\mathbb{P}(A|g, k) \mathbb{P}(g|k)}{\mathbb{P}(A|k)}. \quad (8)$$

Because we have expressions for $\mathbb{P}(A|g, k)$ and $\mathbb{P}(g|k)$ (and because $\mathbb{P}(A|k) \propto 1$), we can use (8) to sample from the posterior distribution $\mathbb{P}(g|A, k)$.

B. Main Model: Unspecified Number of Groups

In our main model for hierarchical core-periphery structure, we suppose that the number k of groups is unspecified. For this case, as in [1], we use a Poisson prior distribution on k with mean 1. Namely,

$$\mathbb{P}(k) = \frac{e^{-1}}{(k-1)!}. \quad (9)$$

We then have

$$\mathbb{P}(g, k|A) = \mathbb{P}(k) \mathbb{P}(g|A, k). \quad (10)$$

Using the expression (10), in Section IV, we derive our main MCMC algorithm for sampling from the posterior distribution (10) and prove that the stationary distribution of a slightly-modified version of this algorithm is the same as (10). In Section IV A 3, we discuss the required modifications of our main MCMC algorithm.

IV. STATISTICAL-INFERENCE APPROACH

To sample from the posterior distribution (10), we use an MCMC method that is similar to the ones in [1].

In Sections IV A, IV B, and IV C, we introduce our MCMC method (see Algorithm 4). To prove that the stable distribution of a slightly-modified version of Algorithm 4 is the same as the desired posterior distribution (10), we introduce versions of Algorithm 4 that do not include certain types of moves and prove intermediate results involving their stable distributions. In Section IV D, we consider Algorithm 6, which is an MCMC algorithm for a fixed number of groups. In Section IV E, we consider Algorithm 7, which is similar to Algorithm 4 but (1) allows the number of groups to vary and (2) does not allow one class of moves that we consider in Algorithm 4. In Section IV F, we prove that the stable distribution of a slightly-modified version of Algorithm 4 is the same as the desired posterior distribution (10).

A. Our Main MCMC Algorithm

We begin by presenting the three types of MCMC moves in Algorithm 4.

1. Standard Moves

The first type of MCMC move, which we call a *standard move* (see Algorithm 1), is a move that adds a node-layer to a group, removes a node-layer from a group, or removes an empty group (i.e., a group that has no nodes). In this type of move, we first uniformly randomly choose a group r and a layer ℓ . The specific move that we propose is different for the first layer $\ell = 1$ and the other layers $\ell \geq 2$.

First consider layer $\ell = 1$. With probability 1/2, we propose a move that adds a node-layer in layer 1 to group r . With probability 1/2, we propose a move that removes a node-layer in layer 1 from group r . If we choose to add a node-layer to a group, we select a node-layer $(i, 1)$ in layer 1 that is not in group r (i.e., $g_{(i,1)}^r = 0$) uniformly

at random from the set of all node-layers $(i, 1)$ in layer 1 that are not in group r . If all node-layers in layer 1 are already in group r , then we do nothing. Analogously, if we choose to remove a node-layer from a group, we select a node-layer $(i, 1)$ in layer 1 that is currently in group r (i.e., $g_{(i,1)}^r = 1$) uniformly at random from the set of all node-layers $(i, 1)$ in layer 1 that are in group r . If no node-layers are in group r , we reduce the number k of groups by 1 by removing group r and shifting the labels of all groups above r down by 1. If group r has no node-layers in layer 1 but at least one node-layer in another layer, then we do nothing.

If layer $\ell \geq 2$, we choose a node i uniformly at random. If node-layer (i, ℓ) is in group r , then we propose a move that removes it from group r . If node-layer (i, ℓ) is not in group r , then we propose a move that adds it to group r . For $\ell \geq 2$, a proposed move cannot remove a group.

Algorithm 1 (Proposal of a standard move)

1. Choose a layer ℓ uniformly at random from $1, \dots, L$.
2. Choose a group r uniformly at random from $1, \dots, k-1$.
3. If $\ell = 1$:
 - (a) With probability $1/2$, we choose to add a node-layer in layer 1 to group r . With probability $1/2$, we choose to remove a node-layer in layer 1 from group r .
 - (b) If we choose to add a node-layer in layer 1 to group r :
 - i. If all node-layers $(i, 1)$ in layer 1 are in group r :
 - A. Do nothing.
 - ii. Otherwise (i.e., if there is at least one node-layer in layer 1 that is not in group r):
 - A. Choose a node-layer $(i, 1)$ that is not in group r uniformly at random from all node-layers $(i, 1)$ that are not in group r .
 - B. Propose a move that adds $(i, 1)$ to group r .
 - (c) If we choose to remove a node-layer in layer 1 from group r :
 - i. If no node-layers (i, ℓ) are in group r :
 - A. Propose a move that removes group r and shifts the labels of all groups above r down by 1.
 - ii. Otherwise, if no node-layers $(i, 1)$ in layer 1 are in group r but group r has at least one node-layer from another layer:
 - A. Do nothing.

- iii. Otherwise (i.e., if group r has at least one node-layer from layer 1):
 - A. Choose a node-layer $(i, 1)$ from group r uniformly at random from all node-layers $(i, 1)$ in group r .
 - B. Propose a move that removes $(i, 1)$ from group r .

4. Otherwise (i.e., if $\ell \geq 2$):

- (a) Choose a node i uniformly at random from $1, \dots, n$.
 - i. If (i, ℓ) is in group r :
 - A. Propose a move that removes (i, ℓ) from group r .
 - ii. If (i, ℓ) is not in group r :
 - A. Propose a move that adds (i, ℓ) to group r .

2. Group-Addition Moves

Our second type of MCMC move is a *group-addition move* (see Algorithm 2). This type of move increases the number k of groups by 1.

Algorithm 2 (Proposal of a group-addition move)

1. Choose a group r uniformly at random from $1, \dots, k$.
2. Propose a move that increases the labels of all groups r and higher by 1, creates a new empty group with the label r , and increases the value of k by 1.

3. Multi-Node Moves

Our third type of MCMC move is a *multi-node move* (see Algorithm 3). This type of move changes more than one group assignment at a time. For a layer ℓ and two subsets \mathcal{G}_1 and \mathcal{G}_2 of the groups $\{1, \dots, k-1\}$, we propose a new group assignment g' that satisfies

$$(g')_{(i,\ell')}^r = \begin{cases} \delta_{\mathcal{G}_2, r}, & \ell' = \ell \text{ and } \delta_{\mathcal{G}_1, (i, \ell')} = 1 \\ \delta_{\mathcal{G}_1, r}, & \ell' = \ell \text{ and } \delta_{\mathcal{G}_2, (i, \ell')} = 1 \\ g_{(i,\ell')}^r, & \text{otherwise,} \end{cases} \quad (11)$$

where

$$\delta_{\mathcal{G}, r} = \begin{cases} 1, & r \in \mathcal{G} \\ 0, & \text{otherwise} \end{cases}$$

and

$$\delta_{\mathcal{G}, (i, \ell)} = \begin{cases} 1, & g_{(i,\ell)}^r = \delta_{\mathcal{G}, r} \text{ for all } r \in \{1, \dots, k-1\} \\ 0, & \text{otherwise.} \end{cases}$$

Algorithm 3 (Proposal of a multi-node move)

1. Select subsets \mathcal{G}_1 and \mathcal{G}_2 uniformly at random from the groups $\{1, \dots, k-1\}$.
2. Choose a layer ℓ uniformly at random from $1, \dots, L$.
3. Propose a move with a new group assignment g' using (11).

As we discussed in Section III B, we need to slightly modify our main MCMC algorithm (see Algorithm 4) to attain equality of the stationary distribution and the desired posterior distribution (10). Specifically, we need to modify Algorithm 3 by choosing the layer ℓ uniformly from $2, \dots, L$ instead of from $1, \dots, L$. In Section IV F, we prove that the stationary distribution of the modified version of Algorithm 4 coincides with the desired posterior distribution (10) and discuss why we nevertheless use the unmodified version of Algorithm 4 to infer core-periphery structure.

B. Acceptance Probability

In Sections IV A 1, IV A 2, and IV A 3, we discussed three types of MCMC moves. In each step of our MCMC algorithm (see Algorithm 4), we propose a move of one of these three types. After proposing a move from g, k to g', k' , we need to determine whether to accept or reject the move. Due to the design of our MCMC algorithm, using the standard Metropolis–Hastings acceptance [35]

$$\min \left\{ 1, \frac{\mathbb{P}(A|g', k')\mathbb{P}(g'|k')}{\mathbb{P}(A|g, k)\mathbb{P}(g|k)} \right\} \quad (12)$$

would cause the stationary distribution of our Markov chain to differ from the desired posterior distribution (10). Therefore, we slightly modify (12) and instead use the acceptance probability

$$\alpha(g, k \rightarrow g', k') = \min \left\{ 1, \frac{\mathbb{P}(A|g', k')\mathbb{P}(g'|k')}{\mathbb{P}(A|g, k)\mathbb{P}(g|k)} \right\}, \quad (13)$$

where we recall that $F(g|k)$ is given by (6).

C. Statement of our Main MCMC Algorithm

Now that we have discussed the three types of MCMC moves (see Sections IV A 1, IV A 2, and IV A 3) and the acceptance probability (see Section IV B) of a move, we now state Algorithm 4, which gives the MCMC approach that we use to identify hierarchical core–periphery structure in temporal networks.

Let $p \in [0, 1]$ denote the probability that a move is a multi-node move. We use Algorithm 4 to sample from the posterior distribution (10) and identify hierarchical core–periphery structure.

Algorithm 4 (Main MCMC algorithm)

1. Propose a move:
 - (a) With probability p , propose a multi-node move (see Algorithm 3).
 - (b) Otherwise, with probability $1 - \frac{1}{2k(n+1)}$, propose a standard move (see Algorithm 1).
 - (c) Otherwise, propose a group-addition move (see Algorithm 2).
2. Accept the proposed move from g, k to g', k' with the acceptance probability
$$\alpha(g, k \rightarrow g', k') := \min \left\{ 1, \frac{\mathbb{P}(A|g', k')\mathbb{P}(g'|k')}{\mathbb{P}(A|g, k)\mathbb{P}(g|k)} \right\}.$$
3. Otherwise, reject the proposed move.

D. MCMC Algorithm for a Fixed Number of Groups

As we discussed in the introduction of Section IV, we prove that the stationary distribution of a slightly-modified version of Algorithm 4 is the same as the desired posterior distribution (10) by proving similar results for intermediate algorithms that build up to the main result. In this section, we consider a fixed number k of groups. In this case, we use only standard moves (see Section IV A 1) in our MCMC algorithm.

Because we fix k , we slightly modify our algorithm for proposing a standard move (see Algorithm 1). In this modified version of the algorithm, if we choose to remove a node-layer in layer 1 and no node-layers are in group r , we do nothing (instead of removing group r , as we did before). In Algorithm 5, we give our modified algorithm for proposing a standard move.

Algorithm 5 (Proposal of a standard move when we fix the number of groups)

1. Choose a layer ℓ uniformly at random from $1, \dots, L$.
2. Choose a group r uniformly at random from $1, \dots, k-1$.
3. If $\ell = 1$:
 - (a) With probability $1/2$, add a node-layer in layer 1 to group r . With probability $1/2$, remove a node-layer in layer 1 from group r .
 - (b) If we choose to add a node-layer in layer 1 to group r :
 - i. If all node-layers $(i, 1)$ in layer 1 are in group r :

- A. Do nothing.
- ii. Otherwise (i.e., if there is at least one node-layer in layer 1 that is not in group r):
 - A. Choose a node-layer $(i, 1)$ that is not in group r uniformly at random from all node-layers $(i, 1)$ that are not in group r .
 - B. Propose a move that adds $(i, 1)$ to group r .
- (c) If we choose to remove a node-layer in layer 1 from group r :
 - i. If no node-layers $(i, 1)$ in layer 1 are in group r :
 - A. Do nothing.
 - ii. Otherwise (i.e., if group r has at least one node-layer from layer 1):
 - A. Choose a node-layer $(i, 1)$ that is in group r uniformly at random from all node-layers $(i, 1)$ that are in group r .
 - B. Propose a move that removes $(i, 1)$ from group r .
- 4. Otherwise (i.e., if $\ell \geq 2$):
 - (a) Choose a node $i \in \{1, \dots, n\}$.
 - i. If (i, ℓ) is in group r :
 - A. Propose a move that removes (i, ℓ) from group r .
 - ii. If (i, ℓ) is not in group r :
 - A. Propose a move that adds (i, ℓ) to group r .

Because we fix the number k of groups, we slightly modify the acceptance probability (13). The acceptance probability of a move from g to g' for this algorithm is

$$\alpha(g \rightarrow g') = \min \left\{ 1, \frac{\mathbb{P}(A|g', k)F(g'|k)}{\mathbb{P}(A|g, k)F(g|k)} \right\}. \quad (14)$$

In Algorithm 6, we give this algorithm for sampling from the posterior distribution (8).

Algorithm 6 (MCMC algorithm for the case of a fixed number of groups)

- 1. Propose a move:
 - (a) Propose a standard move (see Algorithm 5).
- 2. Accept the proposed move from g to g' with the acceptance probability

$$\alpha(g \rightarrow g') := \min \left\{ 1, \frac{\mathbb{P}(A|g', k)F(g'|k)}{\mathbb{P}(A|g, k)F(g|k)} \right\}.$$
- 3. Otherwise, reject the proposed move.

We now show that the equilibrium distribution of this MCMC process is the same as the desired posterior distribution $\mathbb{P}(g|A, k)$ that we stated in (8). To show this, it is sufficient to show that the MCMC process satisfies ergodicity and detailed balance [35]. To prove ergodicity, we need to show that one can access every state in the system from every other state using a finite sequence of moves. To prove detailed balance, we need to show that the mean rate of $g \rightarrow g'$ moves equals the mean rate of $g' \rightarrow g$ moves at equilibrium. That is, we need to verify that

$$\mathbb{P}(g|A, k)\mathbb{P}(g \rightarrow g') = \mathbb{P}(g'|A, k)\mathbb{P}(g' \rightarrow g). \quad (15)$$

In Algorithm 6, ergodicity clearly holds because we can first remove all node-layers from all groups and then re-add node-layers to attain any desired group assignment g . We thus only need to prove that the MCMC process satisfies detailed balance.

To prove detailed balance, we need to verify (15). We write $\mathbb{P}(g \rightarrow g') = \pi(g \rightarrow g')\alpha(g \rightarrow g')$, where π is the probability of proposing a move and α is the probability of accepting it. This implies that equation (15) is equivalent to

$$\frac{\mathbb{P}(g'|A, k)}{\mathbb{P}(g|A, k)} = \frac{\pi(g \rightarrow g')\alpha(g \rightarrow g')}{\pi(g' \rightarrow g)\alpha(g' \rightarrow g)}. \quad (16)$$

Because $\mathbb{P}(g|A, k) = \frac{\mathbb{P}(A|g, k)\mathbb{P}(g|k)}{\mathbb{P}(A|k)} = \frac{\mathbb{P}(A|g, k)F(g|k)\mathbb{P}(g_{(1)}|k)}{\mathbb{P}(A|k)}$ by (8) and (7) and $\alpha(g \rightarrow g') = \min \left\{ 1, \frac{\mathbb{P}(A|g', k)F(g'|k)}{\mathbb{P}(A|g, k)F(g|k)} \right\}$ by (13), equation (16) is equivalent to

$$\frac{\mathbb{P}(A|g', k)F(g'|k)\mathbb{P}(g'_{(1)}|k)}{\mathbb{P}(A|g, k)F(g|k)\mathbb{P}(g_{(1)}|k)} = \frac{\pi(g \rightarrow g')\mathbb{P}(A|g', k)F(g'|k)}{\pi(g' \rightarrow g)\mathbb{P}(A|g, k)F(g|k)},$$

which in turn is equivalent to

$$\frac{\mathbb{P}(g'_{(1)}|k)}{\mathbb{P}(g_{(1)}|k)} = \frac{\pi(g \rightarrow g')}{\pi(g' \rightarrow g)}. \quad (17)$$

We now show that (17) holds for a standard move $g \rightarrow g'$ that adds node-layer $(i, 1)$ to group r . First, because $\mathbb{P}(g_{(1)}|k) = \prod_{s=1}^{k-1} \frac{n_s^{(1)}!(n-n_s^{(1)})!}{(n+1)!}$, we have

$$\frac{\mathbb{P}(g'_{(1)}|k)}{\mathbb{P}(g_{(1)}|k)} = \prod_{s=1}^{k-1} \frac{n_s'^{(1)}!(n-n_s'^{(1})!}{n_s^{(1)}!(n-n_s^{(1)})!}.$$

By adding a node-layer in layer 1 to group r , we obtain $n_r'^{(1)} = n_r^{(1)} + 1$ and $n_s'^{(1)} = n_s^{(1)}$, which then yields

$$\frac{\mathbb{P}(g'_{(1)}|k)}{\mathbb{P}(g_{(1)}|k)} = \frac{n_r^{(1)} + 1}{n - n_r^{(1)}}.$$

From Algorithms 5 and 6, the probability of proposing the move $g \rightarrow g'$ is

$$\pi(g \rightarrow g') = \frac{1}{L} \times \frac{1}{k-1} \times \frac{1}{2} \times \frac{1}{n - n_r^{(1)}}.$$

Similarly, $\pi(g' \rightarrow g) = \frac{1}{L} \times \frac{1}{k-1} \times \frac{1}{2} \times \frac{1}{n_r^{(1)} + 1}$. Therefore,

$$\frac{\pi(g \rightarrow g')}{\pi(g' \rightarrow g)} = \frac{n_r^{(1)} + 1}{n - n_r^{(1)}} = \frac{\mathbb{P}(g_{(1)}|k)}{\mathbb{P}(g_{(1)}|k')}.$$

The detailed-balance equation (17) is thus satisfied in this instance.

We now verify (17) for a standard move $g \rightarrow g'$ that adds node-layer (i, ℓ) to group r when $\ell \geq 2$. First, $n_r' = n_r^{(1)}$ for all r (because adding a node-layer in layer $\ell \geq 2$ does not affect the group sizes in layer 1). This yields

$$\frac{\mathbb{P}(g_{(1)}|k)}{\mathbb{P}(g_{(1)}|k')} = 1.$$

From Algorithms 5 and 6, the probability of proposing the move $g \rightarrow g'$ is

$$\pi(g \rightarrow g') = \frac{1}{L} \times \frac{1}{k-1} \times \frac{1}{n}.$$

Similarly, $\pi(g' \rightarrow g) = \frac{1}{L} \times \frac{1}{k-1} \times \frac{1}{n}$, so

$$\frac{\pi(g \rightarrow g')}{\pi(g' \rightarrow g)} = 1 = \frac{\mathbb{P}(g_{(1)}|k)}{\mathbb{P}(g_{(1)}|k')}.$$

Consequently, the detailed-balance equation (17) is satisfied.

We omit the proofs of (17) for the cases where $g \rightarrow g'$ removes a node-layer in layer $\ell \geq 1$, as they are extremely similar to the arguments above. Now that we have verified both ergodicity and detailed balance, we see that the equilibrium distribution of Algorithm 6 is the same as the desired posterior distribution (8).

E. Intermediate Algorithm for a Variable Number of Groups

We now allow the number k of groups to vary, and we consider an MCMC algorithm for sampling from the desired posterior distribution (10). In contrast to our main algorithm (see Algorithm 4), this algorithm does not use multi-node moves (see Section IV A 3). The number of groups is allowed to vary, so we use our main algorithms for proposing a standard move (see Algorithm 1) and for proposing a group-addition move (see Algorithm 2). We also again use the acceptance probability

$$\alpha(g, k \rightarrow g', k') = \min \left\{ 1, \frac{\mathbb{P}(A|g', k')F(g'|k')}{\mathbb{P}(A|g, k)F(g|k)} \right\}$$

that we specified previously in (13). In Algorithm 7, we give our MCMC algorithm that samples from the desired posterior distribution (10) without using multi-node moves.

Algorithm 7 (MCMC algorithm with no multi-node moves for the case of a variable number of groups)

1. Propose a move:

- (a) With probability $1 - \frac{1}{2k(n+1)}$, propose a standard move (see Algorithm 1).
- (b) Otherwise, propose a group-addition move (see Algorithm 2).

2. Accept the proposed move from g, k to g', k' with acceptance probability

$$\alpha(g, k \rightarrow g', k') := \min \left\{ 1, \frac{\mathbb{P}(A|g', k')F(g'|k')}{\mathbb{P}(A|g, k)F(g|k)} \right\}.$$

3. Otherwise, reject the proposed move.

Algorithm 7 is the same as Algorithm 4 except that it does not allow multi-node moves.

We now show that the equilibrium distribution of this MCMC process is the same as the desired posterior distribution $\mathbb{P}(g, k|A)$ (see (10)). As in the fixed- k case, ergodicity clearly holds for this MCMC procedure. Therefore, it suffices to prove detailed balance. However, in contrast to the fixed- k case, detailed balance holds only in the limit $n \rightarrow \infty$. Following similar logic to the logic for (15)–(17) for the fixed- k case, to prove detailed balance for the variable- k case, we need to show that

$$\frac{\mathbb{P}(g_{(1)}', k')}{\mathbb{P}(g_{(1)}, k)} = \frac{\pi(g, k \rightarrow g', k')}{\pi(g', k' \rightarrow g, k)}. \quad (18)$$

First suppose that $k = k'$, which occurs when $g, k \rightarrow g', k'$ is a standard move that does not change the number of groups. Algorithms 5 and 1 have the same probability of proposing a specific standard move, so the proposed-move probabilities $\pi(g, k \rightarrow g', k')$ and $\pi(g', k' \rightarrow g, k)$ in Algorithm 7 are (aside from a factor of $1 - \frac{1}{2k(n+1)}$) the same as the probabilities $\pi(g \rightarrow g')$ and $\pi(g \rightarrow g')$, respectively, in Algorithm 6. Additionally, by the definition of conditional probability, $\mathbb{P}(g, k) \propto \mathbb{P}(g|k)$ and $\mathbb{P}(g', k') \propto \mathbb{P}(g'|k')$ with the same proportionality constant. The detailed-balance result (17) for the fixed- k case then implies that

$$\frac{\mathbb{P}(g_{(1)}', k')}{\mathbb{P}(g_{(1)}, k)} = \frac{\pi(g, k \rightarrow g', k')}{\pi(g', k' \rightarrow g, k)},$$

so the detailed-balance equation (18) holds for this case.

Now suppose that $k' \neq k$. We will show that detailed balance holds when $g, k \rightarrow g', k'$ is a group-addition move. Because $\mathbb{P}(g_{(1)}|k) = \prod_{r=1}^{k-1} \frac{n_r^{(1)}!(n - n_r^{(1)})!}{(n+1)!}$ and $\mathbb{P}(k) = \frac{e^{-1}}{(k-1)!}$, we obtain

$$\frac{\mathbb{P}(g_{(1)}', k')}{\mathbb{P}(g_{(1)}, k)} = \frac{(k-1)! \prod_{r=1}^k \frac{n_r'^{(1)}!(n - n_r'^{(1)})!}{(n+1)!}}{k! \prod_{r=1}^{k-1} \frac{n_r^{(1)}!(n - n_r^{(1)})!}{(n+1)!}} = \frac{1}{k(n+1)}.$$

From Algorithms 1, 2, and 7, the proposal probabilities $\pi(g, k \rightarrow g', k')$ and $\pi(g', k' \rightarrow g, k)$ are

$$\pi(g, k \rightarrow g', k') = \frac{1}{L} \times \frac{1}{2k(n+1)} \times \frac{1}{k},$$

$$\pi(g', k' \rightarrow g, k) = \frac{1}{L} \times \left(1 - \frac{1}{2(k+1)(n+1)}\right) \times \frac{1}{k} \times \frac{1}{2},$$

where the expression for $\pi(g', k' \rightarrow g, k)$ follows from the fact that $g', k' \rightarrow g, k$ must be a standard move that removes a group. Therefore,

$$\frac{\pi(g, k \rightarrow g', k')}{\pi(g', k' \rightarrow g, k)} = \frac{1}{k(n+1)} + \Theta\left(\frac{1}{n^2}\right).$$

Because $\frac{\mathbb{P}(g', k')}{\mathbb{P}(g, k)} = \frac{1}{k(n+1)}$, we have that

$$\frac{\mathbb{P}(g', k')}{\mathbb{P}(g, k)} = \frac{\pi(g, k \rightarrow g', k')}{\pi(g', k' \rightarrow g, k)}$$

as $n \rightarrow \infty$. Therefore, the detailed-balance equation (18) holds in the limit $n \rightarrow \infty$.

As with the fixed- k case (see Section IV D), we omit the proof of detailed balance when $g, k \rightarrow g', k'$ is a standard move that removes a group, as it is extremely similar to the proof of detailed balance when $g, k \rightarrow g', k'$ is a group-addition move.

F. Revisiting our Main MCMC Algorithm

Although we proved in Section IVE that the stationary distribution of the MCMC approach in Algorithm 7 is the same as the desired posterior distribution (10) in the limit $n \rightarrow \infty$, in practice, this approach often does not lead to the correct identification of core-periphery structure in temporal networks. This occurs because the posterior distribution $\mathbb{P}(g|A)$ from which we sample using this approach has many local maxima, so the algorithm often becomes stuck at suboptimal maxima. In Figure 4.1, we illustrate the behavior that we commonly see at such suboptimal maxima.

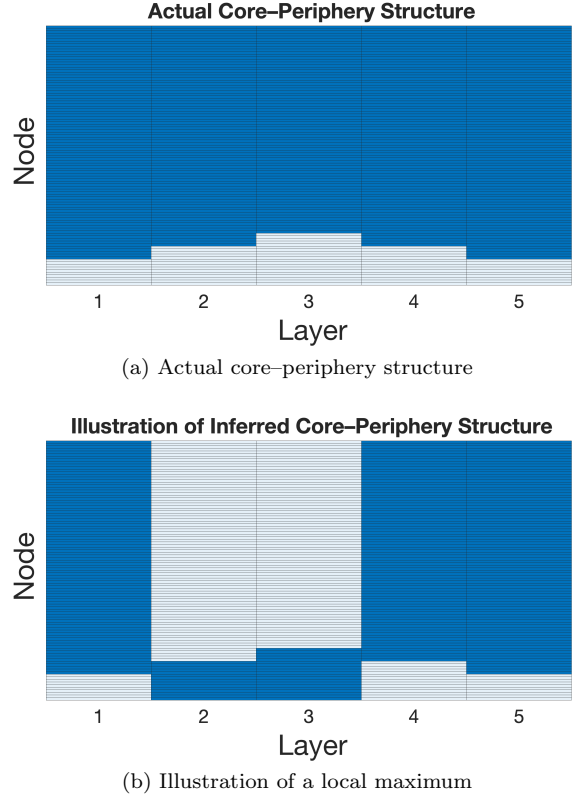


FIG. 1: Heat maps of (a) an example of actual core-periphery structure and (b) an illustration of the permuted group structure that we commonly observe at local maxima of $\mathbb{P}(g|A)$ for a 100-node network with 5 layers. Each rectangle in a heat map corresponds to one node-layer (i, ℓ) . The dark blue rectangles signify the value $g_{(i,\ell)}^1 = 1$, and the light blue rectangles signify the value $g_{(i,\ell)}^1 = 0$.

In this example, we consider a network with 100 nodes and 5 layers. We observe that the group structure of the local maximum is permuted from the actual core-periphery structure in some layers. Specifically, for the nodes in layers $\ell = 2$ and $\ell = 3$, the group assignment g coincides with the group assignment of the actual core-periphery structure if we swap the values 0 and 1 of the group-assignment indicator variables $g_{(i,\ell)}^1$. If $g_{(i,\ell)}^1$ is initially equal to 1, then $g_{(i,\ell)}^1$ becomes 0 after the swap; if $g_{(i,\ell)}^1 = 0$, then $g_{(i,\ell)}^1$ becomes 1 after the swap.

To mitigate this issue, we incorporate multi-node moves into our main MCMC algorithm (see Algorithm 4). Faust [33] showed that including multi-node moves in posterior sampling methods for community detection in temporal networks greatly reduces the frequency at which such methods get stuck at suboptimal local maxima where the inferred community assignments become permuted from the correct community assignments in some layers. This observation motivates our choice to include multi-node moves in our main MCMC algorithm.

We now prove that the stationary distribution of our

main algorithm (see Algorithm 4) coincides with the desired posterior distribution (10). Recall that Algorithm 4 is the same as Algorithm 7 except for the addition of multi-node moves. Including this additional type of move does not impact the detailed-balance calculations in Section IV E (aside from an additional factor of $1 - p$ in all terms), so it suffices to show the detailed-balance equation

$$\frac{\mathbb{P}(g'_{(1)}, k')}{\mathbb{P}(g_{(1)}, k)} = \frac{\pi(g, k \rightarrow g', k')}{\pi(g', k' \rightarrow g, k)} \quad (19)$$

when $g, k \rightarrow g', k'$ and $g', k' \rightarrow g, k$ are multi-node moves. From Algorithms 3 and 4, we have

$$\begin{aligned} \pi(g, k \rightarrow g', k') &= \frac{1}{L} \times p \times \frac{1}{2^{k-1}} \times \frac{1}{2^{k'-1}}, \\ \pi(g', k' \rightarrow g, k) &= \frac{1}{L} \times p \times \frac{1}{2^{k'-1}} \times \frac{1}{2^{k-1}}. \end{aligned}$$

A multi-node move does not change the number of groups, so $k' = k$. Therefore, $\pi(g, k \rightarrow g', k') = \pi(g', k' \rightarrow g, k)$. Recall that we define g' by equation (11) for a multi-node move $g, k \rightarrow g', k'$. From this definition, we see for $\ell \in \{2, \dots, L\}$ that g and g' have the

same group assignments in the first layer, so

$$\mathbb{P}(g'_{(1)}, k') = \mathbb{P}(g_{(1)}, k).$$

Therefore, the detailed-balance equation (19) holds for multi-node moves $g, k \rightarrow g', k'$ for $\ell \in \{2, \dots, k\}$. However, because a multi-node move for $\ell = 1$ nearly always changes the group sizes in layer 1, the detailed-balance equation (19) does not hold for such a move. If we choose to restrict Algorithm 3 to allow multi-node moves only in layers $\ell \in \{2, \dots, k\}$ (as we discussed previously in Section IV A 3), the stationary distribution of our main algorithm (see Algorithm 4) would be the same as the desired posterior distribution (10). However, this choice would cause our MCMC algorithm to become stuck at local extrema with permuted group assignments in the first layer. This would significantly decrease the performance of our approach. Therefore, we do not do this, and we instead allow multi-node moves in all layers.

G. Computation of Acceptance Probability

We now discuss how we compute the acceptance probability (13). Recall from (13) that we must compute

$$\alpha(g, k \rightarrow g', k') = \min \left\{ 1, \frac{\mathbb{P}(A|g', k)F(g'|k)}{\mathbb{P}(A|g, k)F(g|k)} \right\}.$$

It is straightforward to compute $\mathbb{P}(A|g, k)$ from (1). To compute $F(g|k)$, recall from (6) and (4) that

$$\mathbb{P}(g_{(\ell)}^r | g_{(\ell-1)}^r) = \prod_{s=0}^1 \left[\frac{1}{\binom{n_{r;s}^{(\ell-1)}}{c_{r;ss}^{(\ell)}}} \times J(n_s(g_{(\ell-1)}^r) - c_{r;ss}^{(\ell)}, n_s(g_{(\ell-1)}^r)) \right],$$

where

$$F(g|k) = \prod_{\ell=2}^L \prod_{r=1}^{k-1} \mathbb{P}(g_{(\ell)}^r | g_{(\ell-1)}^r)$$

and

$$J(k_1, k_2) = \int_0^1 x^{k_1} \frac{x-1}{x^{k_2+1} - 1} dx.$$

To minimize computational cost, we precompute

$$J(k_1, k_2) = \int_0^1 x^{k_1} \frac{x-1}{x^{k_2+1} - 1} dx$$

for all k_1 and k_2 such that $0 \leq k_1 \leq k_2 \leq n$ using the procedure in Section B.2.1 of [33]. This pre-

computation allows us to avoid needing to repeatedly recompute $J(k_1, k_2)$ when computing (4). [36] We also use analogous arguments to those in equations (4.34)–(4.36) in [33] to avoid directly calculating terms in (6) that will cancel out in the expression (13) for the acceptance probability $\alpha(g, k \rightarrow g', k')$. This reduces the number of times that we need to evaluate $J(k_1, k_2)$. Our implementation of Algorithm 4 is available at <https://github.com/tfaust0196/mhCorePeriphery>.

V. DISCUSSION OF OUR GROUP-ASSIGNMENT APPROACH

We are equipped to discuss an additional rationale behind our choice of group-assignment probability distribution $\mathbb{P}(g|k)$ now that we have introduced Algorithm 4 (see Section IV C, which we use to sample from the desired posterior distribution $\mathbb{P}(g, k|A)$ in (10). Recall from Algorithm 4 and Section IV B that the acceptance probability $\alpha(g, k \rightarrow g', k')$ is

$$\alpha(g, k \rightarrow g', k') = \min \left\{ 1, \frac{\mathbb{P}(A|g', k')F(g', k')}{\mathbb{P}(A|g, k)F(g, k)} \right\}. \quad (20)$$

By (2) and (5), we generate the group assignments for each group independently. Therefore, if we propose a group-addition move that adds an empty group r , the acceptance probability becomes

$$\mathbb{P}(g_{(i,\ell)}^r = 0 \text{ for all } i \in \{1, \dots, n\} \text{ and } \ell \in \{1, \dots, L\}).$$

Consequently, if a generative model is biased against groups with few node-layers, then the acceptance probability (20) is very small. This, in turn, causes an associated statistical-inference method to underestimate the number of groups.

For a monolayer network (i.e., an ordinary graph), one can resolve the above issue by generating the group sizes uniformly at random. With this choice, the probability of generating an empty group is $\frac{1}{n+1}$. However, for a temporal network, it is difficult to choose a generative model that is not biased against groups with few node-layers. In [33], we showed that the commonly-used approach (see, e.g., [37–40]) of evolving group assignments via a discrete-time Markov process (where one bases the group assignment of a node in a given layer on its group assignment in the previous layer) leads to an increased bias against small and large groups in later layers. This, in turn, leads to a strong bias of a generative model against small and large groups in a network. In our context of hierarchical core–periphery structure, this bias makes the acceptance probability (20) of a group-addition move prohibitively small, leading to an underestimation in the number of groups.

Our novel group-assignment approach is much less biased against small and large groups than such Markov-process approaches. This is the case because our approach generates the group assignments for a layer based on all of the previous group assignments in the previous layer, instead of using a discrete-time Markov process to evolve the group assignments of each node individually. (See Sections 4.2.3.3 and 4.3 of [33] for more information.) Therefore, our method is much less likely to underestimate the number of groups in a network.

This discussion illustrates the practical importance of carefully considering potentially undesirable assumptions of the generative models in statistical-inference methods. See [33] for further discussion and examples in the context of community structure.

VI. APPLICATION TO REAL-WORLD NETWORKS

In this section, we apply our hierarchical core–periphery detection method to two real-world networks and discuss the structures that we identify in these networks. In Section VIA, we consider a network of terrorists in the Indian states of Jammu and Kashmir. In Section VI B, we consider a network of co-appearances in the *Luke Gospel*.

A. Jammu–Kashmir Terrorist Network

We first apply our method to a network of links between terrorist organizations in the Indian states of Jammu and Kashmir from 2000 to 2003 [31]. This temporal network consists of $n = 34$ nodes (which represent terrorist organizations) and $L = 4$ layers (which represent years). Applying our hierarchical core–periphery detection method to this network yields $k = 2$ groups and the core–periphery structure in Figure 2. To generate the core–periphery structure in Figure 2, we perform 5 runs of 10^6 steps of our main MCMC algorithm (see Algorithm 4) with the number k of groups initialized to 4, the probability p of a multi-node move set to 10^{-3} , and the initial group assignments selected uniformly at random for each run. We then save the output group assignments every 10^4 steps. For each node-layer (i, ℓ) , we set the group assignment for (i, ℓ) to be the most frequent group assignment among each of the saved group assignments (across all runs).

To demonstrate that the detected core–periphery structure is reasonable, we plot heat maps (see Figure 3) of the adjacency matrices $A^{(\ell)}$ for each layer ℓ . In these heat maps, we permute the rows and columns so that all node-layers (i, ℓ) with $g_{(i,\ell)}^1 = 1$ preferentially occur earlier. We also include a dividing line between the node-layers with $g_{(i,\ell)}^1 = 1$ and the node-layers with $g_{(i,\ell)}^1 = 0$. In Figure 3, we show these heat maps, and we can see that the node-layers with $g_{(i,\ell)}^1 = 1$ (i.e., the core node-layers) are densely connected to other nodes with $g_{(i,\ell)}^1 = 1$ and that the node-layers with $g_{(i,\ell)}^1 = 0$ (i.e., the peripheral node-layers) are sparsely connected to all other node-layers.

B. Literary Co-Appearance Network

We also apply our method to a network of co-appearances in the *Luke Gospel* [32]. This temporal network consists of $n = 76$ nodes (which represent characters) and $L = 5$ layers (which represent non-overlapping ranges of 4 consecutive chapters). We place an edge between two nodes in a given layer if the two associated characters encounter each other in those chapters. As in Section VIA, we perform 5 runs of 10^6 steps of our main

MCMC algorithm (see Algorithm 4) with the number k of groups initialized to 4, the probability p of a multi-node move set to 10^{-3} , and the initial group assignments selected uniformly at random for each run. We then save the output group assignments every 10^4 steps. In contrast to the results from Section VI A, the inferred group assignments differ greatly between runs. Therefore, unlike for the Jammu–Kashmir terrorist network, we cannot reasonably choose to set the group assignment for each node-layer (i, ℓ) to be the most frequent group assignment across all runs.

One of the reasons that different runs yield different group assignments is that group assignments are permuted between layers in two of the five runs. In Figure 4, we illustrate this with an example of such a run.

Recall from Section IV F that we commonly observe permutations of group assignments between layers in local maxima of the MCMC algorithm without multi-node moves. This suggests that multi-node moves are less effective at avoiding such extrema for the *Luke Gospel* literary co-appearance network than for the Jammu–Kashmir terrorist network. We do not have an explanation for why multi-node moves are less effective for this example. However, the inferred core–periphery structure for each of the layers appears to be plausible. When we permute the adjacency matrices according to the core–periphery structure in Figure 4 (as in Section VI A), the densities of the edges between node-layers depend on the groups that the node-layers are in.

In runs where group assignments are not permuted between layers, we detect reasonable core–periphery structure. In particular, one of the runs of our core–periphery detection method on the *Luke Gospel* literary co-appearance network yields $k = 3$ groups and the core–periphery structure in Figure 5. Observe that the group assignments are not permuted between layers (except possibly for the last layer).

To demonstrate that the detected core–periphery structure in Figure 5 is reasonable, we plot heat maps (see Figure 6) of the adjacency matrices $A^{(\ell)}$ for each layer ℓ . In these heat maps, we permute the rows and columns so that all node-layers (i, ℓ) with $g_{(i, \ell)}^1 = 1$ and $g_{(i, \ell)}^2 = 1$ appear earliest, followed by node-layers (i, ℓ) with $g_{(i, \ell)}^1 = 0$ and $g_{(i, \ell)}^2 = 1$, node-layers (i, ℓ) with $g_{(i, \ell)}^1 = 1$ and $g_{(i, \ell)}^2 = 0$, and finally node-layers (i, ℓ) with $g_{(i, \ell)}^1 = 0$ and $g_{(i, \ell)}^2 = 0$. We observe that the densities of the edges between node-layers depend on the groups that the node-layers are in. For example, in layers 2–4, node-layers with group assignments $g_{(i, \ell)}^1 = 1$ and $g_{(i, \ell)}^2 = 0$ tend to be densely connected to node-layers with group assignments $g_{(i, \ell)}^1 = 0$ and $g_{(i, \ell)}^2 = 0$ but sparsely connected to node-layers with group assignments $g_{(i, \ell)}^1 = 1$ and $g_{(i, \ell)}^2 = 1$. However, the validity of the inferred

core–periphery structure is less evident than the inferred core–periphery structure of the Jammu–Kashmir terrorist network. We hypothesize that this is because the *Luke Gospel* literary co-appearance network is less dense than the Jammu–Kashmir terrorist network.

VII. CONCLUSIONS AND DISCUSSION

We proposed a method to identify hierarchical core–periphery structure in temporal networks. We applied this method to two real-world networks and obtained reasonable inferred structures when our MCMC method converged.

By using the group-evolution probability distribution from [33] (instead of a group-evolution probability distribution that is based on a discrete-time Markov process), our Markov-chain Monte Carlo (MCMC) approach for statistical inference is able to mitigate the underestimation of the number of groups in networks in the detection of hierarchical core–periphery structure. Additionally, by using multi-node moves, we sped up the convergence to the inferred core–periphery structure.

There are a variety of ways to build on our work. The primary weakness of our approach is the high computational cost of each iteration in our MCMC approach, which (despite the use of multi-node moves to reduce the number of iterations to achieve convergence) makes it prohibitive to apply our method to networks with many nodes or layers. Therefore, it is important to develop and implement more computationally efficient methods to identify hierarchical core–periphery structure in temporal networks and more generally in multilayer networks.

We hypothesized in Section VIB that our method identifies hierarchical core–periphery structure less accurately for sparse networks than for dense networks. It is important to examine the performance of our method on synthetic networks with different densities to better understand the effect of density on it. Finally, we emphasize that there have been very few studies of core–periphery structure in temporal and multilayer networks — a situation that contrasts with the voluminous analysis of temporal and multilayer community structure [41, 42] — and such efforts deserve more attention. We expect that such studies will yield both theoretical and practical insights.

ACKNOWLEDGEMENTS

We thank Arash Amini and Grace Li for helpful discussions. TYF was supported by the National Science Foundation Graduate Research Fellowship Program (under Grant No. DGE-2034835).

[1] A. Polanco and M. E. J. Newman, Hierarchical core–periphery structure in networks, *Physical Review E* **108**,

024311 (2023).

[2] M. E. J. Newman, *Networks*, 2nd ed. (Oxford University Press, Oxford, UK, 2018).

[3] S. Fortunato, *Network Community Detection* (Cambridge University Press, Cambridge, UK, 2025).

[4] R. A. Rossi and N. K. Ahmed, Role discovery in networks, *IEEE Transactions on Knowledge and Data Engineering* **27**, 1112 (2015).

[5] P. Csermely, A. London, L.-Y. Wu, and B. Uzzi, Structure and dynamics of core/periphery networks, *Journal of Complex Networks* **1**, 93 (2013).

[6] P. Rombach, M. Porter, J. Fowler, and P. Mucha, Core-periphery structure in networks (revisited), *SIAM Review* **59**, 619 (2017).

[7] E. Yanchenko and S. Sengupta, Core-periphery structure in networks: A statistical exposition, *Statistics Surveys* **17**, 42 (2023).

[8] M. Granovetter, The strength of weak ties: A network theory revisited, *Sociological Theory* **1**, 201 (1983).

[9] H. C. White, S. A. Boorman, and R. L. Breiger, Social structure from multiple networks. I. Blockmodels of roles and positions, *American Journal of Sociology* **81**, 730 (1976).

[10] P. Doreian, Structural equivalence in a psychology journal network, *Journal of the American Society for Information Science* **36**, 411 (1985).

[11] C. L. Willis and S. J. McNamee, Social networks of science and patterns of publication in leading sociology journals, 1960 to 1985, *Knowledge* **11**, 363 (1990).

[12] W. G. Roy, The unfolding of the interlocking directorate structure of the United States, *American Sociological Review* **48**, 248 (1983).

[13] S. W. Williams, Internal colonialism, core-periphery contrasts and devolution: An integrative comment, *Area* **9**, 272 (1977).

[14] S. H. Lee, M. Cucuringu, and M. A. Porter, Density-based and transport-based core-periphery structures in networks, *Physical Review E* **89**, 032810 (2014).

[15] J. Fournet and A. Barrat, Contact patterns among high school students, *PLoS ONE* **9**, e107878 (2014).

[16] I. Morer, A. Cardillo, A. Díaz-Guilera, L. Prignano, and S. Lozano, Comparing spatial networks: A one-size-fits-all efficiency-driven approach, *Physical Review E* **101**, 042301 (2020).

[17] S. H. Lee, J. M. Magallanes, and M. A. Porter, Time-dependent community structure in legislation cosponsorship networks in the Congress of the Republic of Peru, *Journal of Complex Networks* **5**, 127 (2016).

[18] Z. P. Neal, A sign of the times? Weak and strong polarization in the U.S. Congress, 1973–2016, *Social Networks* **60**, 103 (2020).

[19] P. Holme and J. Saramäki, Temporal networks, *Physics Reports* **519**, 97 (2012).

[20] P. Holme, Modern temporal network theory: A colloquium, *The European Physical Journal B* **88**, 234 (2015).

[21] P. Holme and J. Saramäki, *Temporal Network Theory*, 2nd ed. (Springer, Cham, Switzerland, 2023).

[22] M. Kivelä, A. Arenas, M. Barthelemy, J. P. Gleeson, Y. Moreno, and M. A. Porter, Multilayer Networks, *Journal of Complex Networks* **2**, 203 (2014).

[23] X. Zhang, T. Martin, and M. E. J. Newman, Identification of core-periphery structure in networks, *Physical Review E* **91**, 032803 (2015).

[24] R. J. Gallagher, J.-G. Young, and B. F. Welles, A clarified typology of core-periphery structure in networks, *Science Advances* **7**, eabc9800 (2021).

[25] K. Bergermann, M. Stoll, and F. Tudisco, A nonlinear spectral core–periphery detection method for multiplex networks, *Proceedings of the Royal Society A: Mathematical, Physical and Engineering Sciences* **480**, 20230914 (2024).

[26] K. Bergermann and F. Tudisco, Core-periphery detection in multilayer networks, *arXiv preprint*, 2412.04179 (2024).

[27] J. Nie, Q. Xuan, D. Gao, and Z. Ruan, An effective method for profiling core–periphery structures in complex networks, *Physica A: Statistical Mechanics and its Applications* **669**, 130618 (2025).

[28] F. Hashemi and A. Behrouz, A unified core structure in multiplex networks: From finding the densest subgraph to modeling user engagement, in *Proceedings of the 30th ACM SIGKDD Conference on Knowledge Discovery and Data Mining*, KDD '24 (Association for Computing Machinery, New York, NY, USA, 2024) pp. 1028–1039.

[29] For illustrations of the types of structures that one can generate using this hierarchical core–periphery structure, see Figure 1 of [1].

[30] T. P. Peixoto, *Descriptive vs. Inferential Community Detection in Networks: Pitfalls, Myths and Half-Truths*, Elements in the Structure and Dynamics of Complex Networks (Cambridge University Press, Cambridge, UK, 2023).

[31] S. Saxena, K. Santhanam, and A. Basu, Application of Social Network Analysis (SNA) to terrorist networks in Jammu & Kashmir, *Strategic Analysis* **28**, 84 (2004).

[32] A. J. Holanda, M. Matias, S. M. S. P. Ferreira, G. M. L. Benevides, and O. Kinouchi, Character networks and book genre classification, *International Journal of Modern Physics C* **30**, 1950058 (2019).

[33] T. Y. Faust, *Inference and Size Localization of Mesoscale Structures in Temporal Networks*, Ph.D. thesis, University of California, Los Angeles, <https://escholarship.org/uc/item/8q68n9v4> (2025).

[34] For a full discussion of the approach that we use to generate $g_{(\ell)}^r$ from $g_{(\ell-1)}^r$, see Section 4.2.3.3 and Appendix B.2 of [33].

[35] C. P. Robert and G. Casella, The Metropolis–Hastings algorithm, in *Monte Carlo Statistical Methods* (Springer, Heidelberg, Germany, 2004) pp. 267–320, chapter 7.

[36] If n is sufficiently large, the integral $J(k_1, k_2)$ can become very small, which causes finite-precision issues and thereby leads to inaccurate results when computing $J(k_1, k_2)$ using the procedure in Section B.2.1 of [33]. To mitigate this problem, we use the approximation

$$\frac{J(k_1 + 1, k_2)}{J(k_1, k_2)} \approx 1$$

for large k_1 and k_2 . In particular, for fixed k_2 , we set the computed values of $J(k_1, k_2)$ to $\exp(-16)$ for all $k_1 \geq k'_1$, where k'_1 is the smallest k'_1 such that $J(k'_1, k_2) < \exp(-16)$.

[37] T. Yang, Y. Chi, S. Zhu, Y. Gong, and R. Jin, Detecting communities and their evolutions in dynamic social networks—A Bayesian approach, *Machine Learning* **82**, 157 (2011).

[38] A. Ghasemian, P. Zhang, A. Clauset, C. Moore, and L. Peel, Detectability thresholds and optimal algorithms for community structure in dynamic networks, *Physical Review X* **6**, 031005 (2016).

- [39] C. Matias and V. Miele, Statistical clustering of temporal networks through a dynamic stochastic block model, *Journal of the Royal Statistical Society Series B: Statistical Methodology* **79**, 1119 (2016).
- [40] M. Bazzi, L. G. S. Jeub, A. Arenas, S. D. Howison, and M. A. Porter, A framework for the construction of generative models for mesoscale structure in multilayer net-works, *Physical Review Research* **2**, 023100 (2020).
- [41] G. Rossetti and R. Cazabet, Community discovery in dynamic networks: A survey, *ACM Computing Surveys* **51**, 35 (2018).
- [42] X. Huang, D. Chen, T. Ren, and D. Wang, A survey of community detection methods in multilayer networks, *Data Mining and Knowledge Discovery* **35**, 1 (2021).

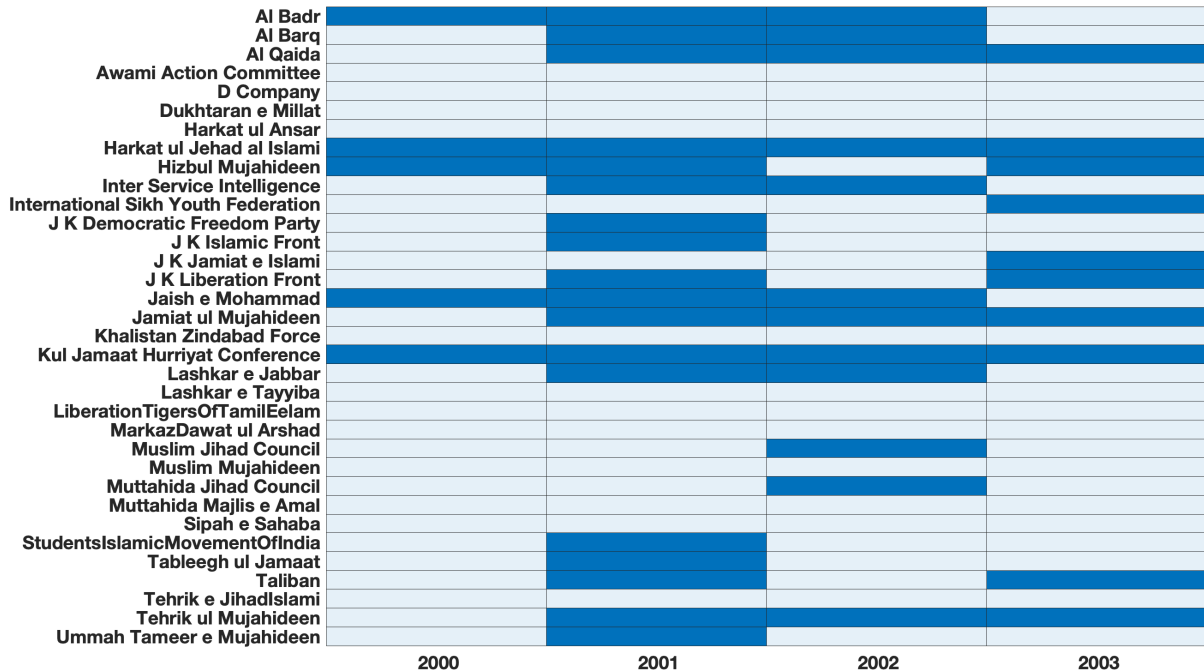


FIG. 2: The inferred core-periphery structure in the Jammu-Kashmir terrorist network. The dark blue rectangles signify the value $g_{(i,\ell)}^1 = 1$, and light blue rectangles signify the value $g_{(i,\ell)}^1 = 0$. The horizontal axis indicates years and the vertical axis indicates terrorist organizations.

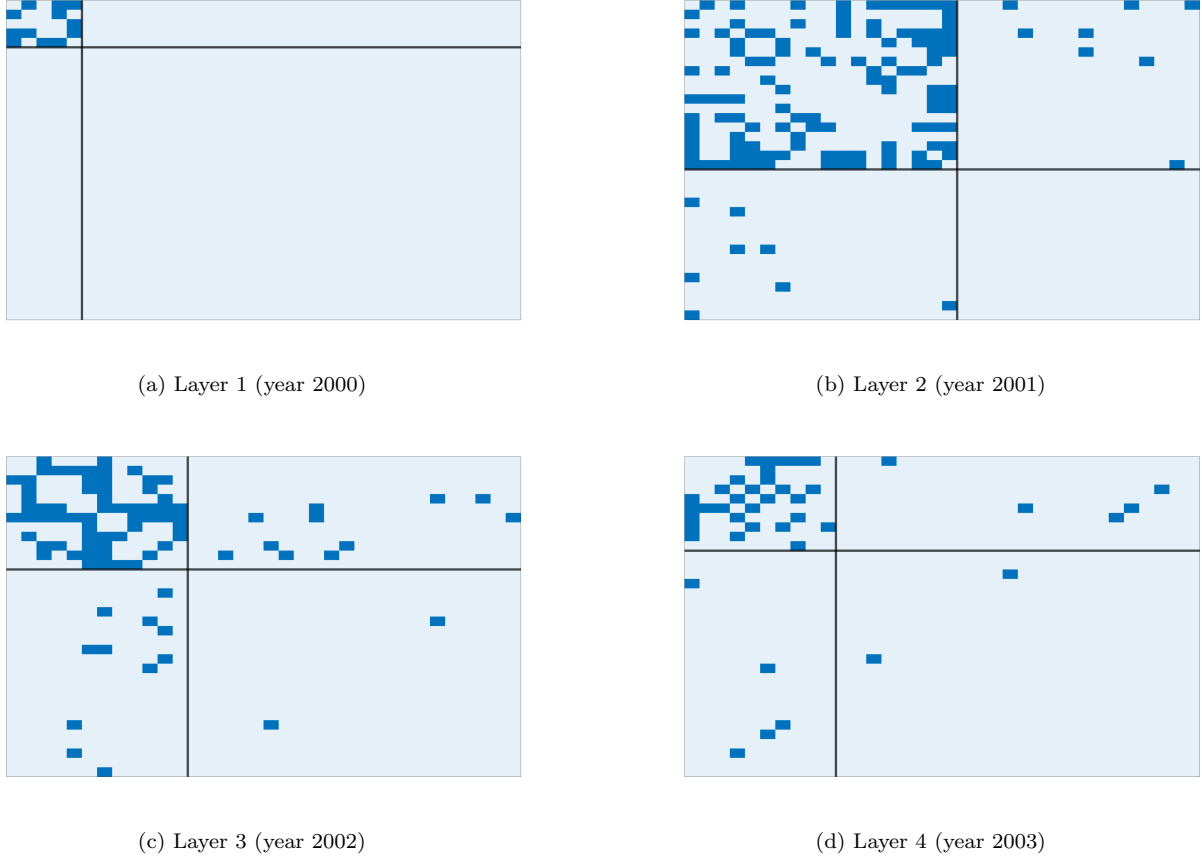


FIG. 3: Permuted adjacency matrices to illustrate the inferred core–periphery structure in the Jammu–Kashmir terrorist network. We show (a) layer 1 (the year 2000), (b) layer 2 (the year 2001), (c) layer 3 (the year 2002), and (d) layer 4 (the year 2003).

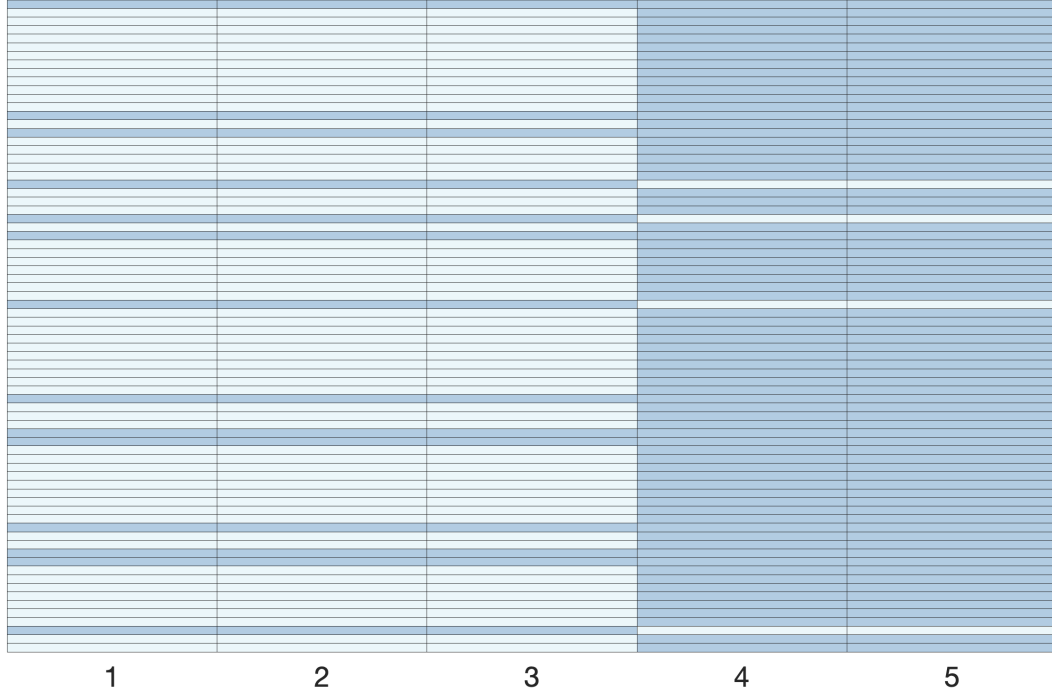


FIG. 4: The inferred core–periphery structure from one run of Algorithm 4 applied to the *Luke Gospel* literary co-appearance network. The light blue rectangles signify the value $g_{(i,\ell)}^1 = 1$, and the dark blue rectangles signify the value $g_{(i,\ell)}^1 = 0$. The horizontal axis indicates non-overlapping ranges of 4 consecutive chapters and the vertical axis indicates characters.

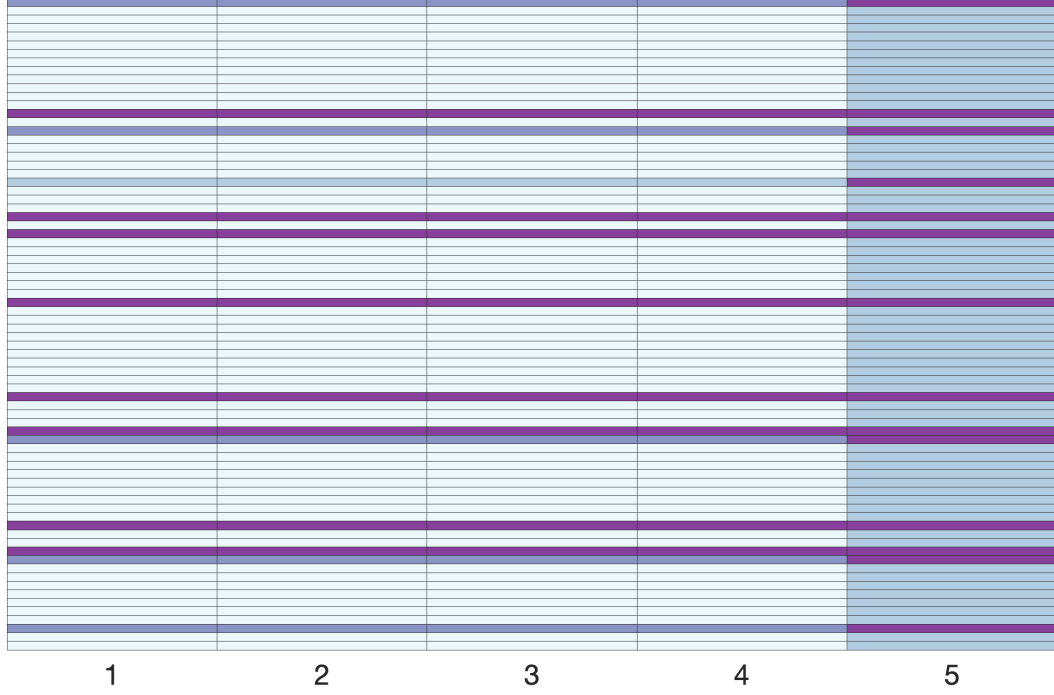


FIG. 5: The inferred core–periphery structure from one run of Algorithm 4 applied to the *Luke Gospel* literary co-appearance network. The light blue rectangles signify the values $g_{(i,\ell)}^1 = 0$ and $g_{(i,\ell)}^2 = 0$, the dark blue rectangles signify the values $g_{(i,\ell)}^1 = 1$ and $g_{(i,\ell)}^2 = 0$, the light purple rectangles signify the values $g_{(i,\ell)}^1 = 0$ and $g_{(i,\ell)}^2 = 1$, and the dark purple rectangles signify the values $g_{(i,\ell)}^1 = 1$ and $g_{(i,\ell)}^2 = 1$. The horizontal axis indicates non-overlapping ranges of 4 consecutive chapters and the vertical axis indicates characters.

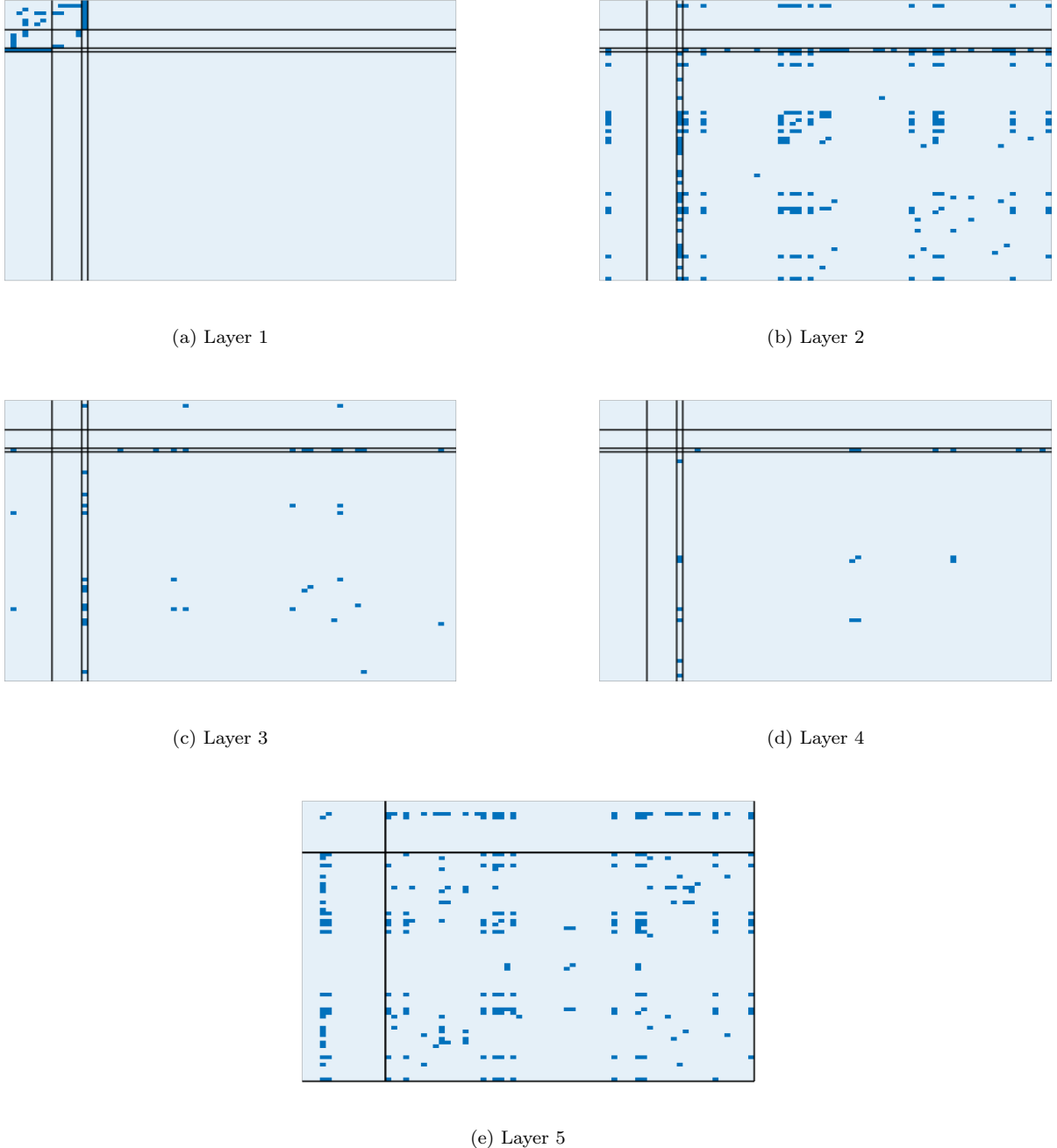


FIG. 6: Permuted adjacency matrices to illustrate the inferred core-periphery structure in the *Luke Gospel* literary co-appearance network. We show (a) layer 1, (b) layer 2, (c) layer 3, (d) layer 4, and (e) layer 5.